Evaluation of leaf-level optical properties employed in land surface models - example with CLM 5.0

Titta Majasalmi[1], Ryan M. Bright[1]

[1]Norwegian Institute of Bioeconomy Research (NIBIO), Box 115, 1433 Ås, Norway

5 *Correspondence to*: Titta Majasalmi (titta.majasalmi@nibio.no)

Abstract

Vegetation optical properties have a direct impact on canopy absorption and scattering and are thus needed for modeling surface fluxes. Although Plant Functional Type (PFT) classification varies between different land surface models (LSMs), their optical properties must be specified. The aim of this study is to revisit the 'time-invariant optical properties table' of the

10 Simple Biosphere (SiB) model (later referred as 'SiB-table') presented 30-years ago by Dorman and Sellers (1989) which has since become adopted by many LSMs. This revisit was needed as much of the data underlying the SiB-table was not formally reviewed or published or was based on older papers or personal communications (i.e. the validity of the optical property source data cannot be inspected due to missing data sources, outdated citation practices, and varied estimation methods). As many of today's LSMs (e.g. Community Land Model (CLM), Jena Scheme of Atmosphere Biosphere Coupling in Hamburg (JSBACH),

15 and Joint UK Land Environment Simulator (JULES)) either rely on the optical properties of the SiB-table or lack references altogether for those they do employ, there is a clear need to assess (and confirm or correct) the appropriateness of those being used in today's LSMs. Here, we use various spectral databases to synthesize and harmonize the key optical property information of PFT classification shared by many leading LSMs. For forests, such classifications typically differentiate PFTs by broad geo-climatic zones (i.e. tropical, boreal, temperate) and phenology (i.e. deciduous vs. evergreen). For short-statured

20 vegetation, such classifications typically differentiate between crops and grasses and by photosynthetic pathway. Using the PFT classification of the CLM (version 5) as an example, we found the optical properties of the visible band (VIS; 400-700 nm) to be appropriate. However, in the near-infrared and shortwave infrared bands (NIR+SWIR; e.g. 701-2500 nm, referred as 'NIR') notable differences between CLM default and measured estimates were observed, thus suggesting that NIR optical properties need updating in the model. For example, for conifer PFTs, the measured mean needle albedo estimates in NIR were

25 62% and 78% larger than the CLM default parameters, and for PFTs with flat-leaves, the measured mean leaf albedo values in NIR were 20%, 14% and 19% larger than the CLM defaults. We also found that while the CLM5 PFT-dependent leaf angle definitions were sufficient for forested PFTs and grasses, for crop PFTs the default parameterization appeared too vertically oriented thus warranting an update. In addition, we propose using separate bark reflectance values for conifer and deciduous PFTs and introduce the concept and application of 'photon recollision probability' (p). The p may be used to upscale needle

30 spectra into shoot spectra to meet the common assumption that foliage is located randomly within the canopy volume (behind canopy radiative transfer calculation) to account for multiple scattering effects caused by needles clustered into shoots.

1 Introduction

Vegetation optical properties have a direct impact on canopy absorption and scattering and are thus needed for modeling surface fluxes. All land surface models (LSMs) have modules to simulate radiation transfer (later referred as 'RT') of surfaces. Although there are many types of canopy RT models with varying complexities - from light extinction algorithms to those

5 applying turbid-medium and geometric-optical methods - they must specify the following: optical properties (i.e. reflectance 'R' and transmittance 'T') of canopy elements such as foliage and bark, canopy foliage density (e.g. Leaf Area Index (LAI, m^2/m^2), and vegetation spatial ordering (e.g. Leaf Inclination Angle, LIA, angle between the leaf surface normal and the zenith). At present, most LSMs are limited to one-dimensional radiative exchange relying on solutions derived from two-stream approximations based on plane-parallel turbid media assumptions (Loew et al., 2014, Yuan et al., 2017).

30 years ago, Dorman and Sellers (1989) presented a 'time-invariant optical properties table' for the Simple Biosphere (SiB) model (later referred as 'SiB-table' or 'SiB-classes') which was compiled using available data and field notes of the time. To the best of our knowledge, some of this data, however, was either never subjected to formal peer-review and published (e.g. Miller, 1972; Klink and Willmot, 1985) or was based on earlier research citing even older papers or personal communications

15 (i.e. the validity of the source data cannot be examined due to a lack of transparency). As many of today's LSMs (e.g. Community Land Model (CLM) (Bonan et al., 2002), land surface model developed at the Institut d'Astronomie et de Ge´ophysique Georges Lemaıˆtre (IAGL) (Ridder, 1997), Jena Scheme of Atmosphere Biosphere Coupling in Hamburg (JSBACH, Reick et al., 2012), and Joint UK Land Environment Simulator (JULES) (Clark et al., 2011) either rely on the original SiB-table optical properties or on undocumented data - there is a clear need to assess (and confirm or correct) the

20 appropriateness of PFT-dependent optical properties by benchmarking to data collected and stored using present-day research norms and documentation standards.

Measurements of R and T of leaves and needles can be achieved using integrating spheres (e.g. Hovi et al., 2017; Lukeš et al., 2013), R of bark and short vegetation (i.e. grasses and crops) using handheld spectrometers (e.g. Lang et al., 2002), and LIA

25 using inclinometers or digital photography (e.g. Ryu et al., 2010)). Measured R and T spectra can be averaged over different wavelength bands (e.g. visible (VIS), 400-700 nm; near-infrared and shortwave infrared (NIR+SWIR, later referred as 'NIR'), 701-2500 nm) required by LSMs, or resampled to correspond with different satellite sensor's band definitions (Asner et al., 1998). Although laboratory measurements of leaf optical properties have been done since the 1960's (Gates et al., 1965), compiling the spectra into public databases with measured other traits and metadata started relatively recently. Today's spectral

30 libraries, such as EcoSIS (EcoSIS, 2017) and SPECCHIO (Hueni et al., 2009), are open databases for storing spectral data from different field campaigns to promote data usage by researchers and model developers. Some reputable example datasets stored in EcoSIS are 'Lopex93' (Hosgood et al., 1993) and 'Angers'(Jacquemound et al., 2003): Lopex93 and Angers contain data for species with flat leaves. For needleleaved species, spectral data is available from SPECCHIO. Reflectance spectra of

different types of (hemi-)boreal grass species communities and tree bark are available e.g. from Estonian research database by Lang et al. (2002). Although much spectral data exists and are freely available, the earlier spectral datasets suffer from not being available online (e.g. data for 26 species from herbs to trees measured in Mississippi and Kansas, USA (Knapp and Carter, 1998) or having limited wavelength range (e.g. BOREAS, comprised North American tree species, was limited to the

5   wavelength range of 400–1100 nm (Middleton et al., 1997)).

Similar with the developments of spectral databases, a wealth of information surrounding forest foliage *LIA* (°) has become available in recent years owed to new measurement techniques (e.g. Ryu et al., 2010). *LIA* is needed for separating foliage area into sunlit and shaded parts as foliage responses to diffuse and direct solar radiation differ (Gu et al., 2002), and for RT

10   model inversion (Combal et al., 2003). While measuring *LIA* of grasses and crops is relatively straightforward and has been conducted since 1960 using inclined point quadrats (Warren Wilson, 1960), methods for measuring tree foliage *LIA* have been lacking due to problems applying them to tall forest canopies (i.e. the high cost of measurements and inability to reproduce them). At present, a state-of-the-art method for determining *LIA*s is based on digital photography which allows robust, non-destructive measurements (i.e. reproducible data) with low cost. In the absence of measured data, estimates regarding leaf

15   angle distributions have often been obtained using modeling or assumed spherical (e.g. Oker-Blom and Kellomäki, 1982; Goudriaan, 1988). Based on compilation of measured and published data, we assess the appropriateness of the PFT-dependent *LIA* parameterization used by today's LSMs.

In addition to providing *R* and *T* assessment for different PFTs, another RT related enhancement may be introduced - the

20   concept of 'photon recollision probability' (*p*). The *p* is a spectrally invariant structural property which can be interpreted as the probability by which a photon scattered (reflected or transmitted) from a leaf or needle in the canopy will interact within the canopy again (Smolander and Stenberg, 2005). In a canopy composed of leaves, a photon scattered from a leaf will not re-interact with the same leaf; however, in a canopy composed of shoots, a photon scattered out from a shoot may have interacted with the needles forming the shoot multiple times. Thus, the common assumption that foliage is located randomly within the

25   canopy volume is violated by conifer canopies due to foliage clumping into shoots causing multiple scattering to occur (Norman and Jarvis, 1975). However, the violation may be mitigated by changing the basic unit from a needle to a shoot (Nilson and Ross, 1996), by upscaling needle spectra into shoot spectra based on shoot geometry (= *p*) (Rautiainen et al., 2012), and by simply replacing needle albedo with shoot albedo in the RT calculation. Shoot spectral albedos are considerably smaller than needle albedos (Rautiainen et al., 2012), which will be also demonstrated in this study.

30

There is large variation in the way optical properties can be defined (e.g. species composition) and measured (e.g. measuring device and its wavelength range). Therefore, the main objective of this study is not to provide 'final truth' regarding PFTs optical properties; rather, our aim is to assess their appropriateness by benchmarking to data collected and stored using present-day research norms, reviewed and synthesized here. Specifically, our objectives are to: 1) verify the PFT-dependent optical

properties used in today's LSMs using the CLM PFT classification and optical property look-up table as an example, 2) suggest an approach to account for within-shoot multiple scattering of conifers in RT calculation; and 3) assess the appropriateness of the *LIA* specification included in the CLM's (e.g. v5) optical properties table. Three supplementary files are provided to inspect the observed variation, and to recalculate the PFT-dependent means following different PFT definitions: Our recommendation

5 for enhancing CLM5 optical properties table ('S1_CLM5.pdf'), and two source files ('S2_OP.csv' and 'S3_LIA.csv'), which contain species mean optical property (i.e. *T*, *R* and *leaf albedo* and for conifers *shoot albedo*) values over the VIS and NIR bands, and species mean *LIA*s (in degrees and departure from spherical + classic leaf angle type) along with references to raw data.

2 Materials and Methods

10 ### 2.1 Pedigree of the CLM -table

The following briefly describes the composition of the optical properties table used by today's CLM versions that is used as an example PFT-classification in this paper. The SiB-table by Dorman and Sellers (1989) was partly reused by (Bonan et al., 2002) to suit the needs of the CLM (**Table 1.**). Bonan et al. (2002) assigned properties of SiB-table class 1 'broadleaved-evergreen trees' ('BET') and SiB-table class 2, 'broadleaved-deciduous trees' (BDT), for CLM 'BET tropical', 'BET -

15 temperate', 'BDT temperate', 'BDT boreal', 'BDT tropical', and for PFTs containing 'broadleaved-deciduous shrubs' (BDS) (i.e. 'BDS temperate' and 'BDS boreal'). The leaf angle specification (as departure from spherical, χ_L, i.e. 1= planophile, -1= erectophile, and 0= spherical) for both BET PFTs was set to 0.10, and for temperate and boreal BDTs and BDSs to 0.25. However, for 'BDT tropical', the leaf angle was set 0.01. The SiB-class 4 'Needleleaf-evergreen trees' (NET) and class 5 'Needleleaf-deciduous trees' (NDT) were used to form CLM PFTs 'NET temperate' and 'NET boreal,' 'NDT boreal' and

20 'broadleaf-evergreen shrubs (BES) temperate'. Based on CLM grass and crop χ_L of -0.30, it seems that SiB-table class 7, 'groundcover' was used to parameterize the optical properties of grasses and crops in Bonan et al. (2002). However, in later CLM versions such as in CLM5 (**Table 1.**), the optical properties of grass and crop PFTs were referenced to Asner et al. (1998), in which the estimates are presented only for spectral subsets following different satellite sensor bandwidths (e.g. AVHRR bands 1 (VIS, 550-700 nm) and 2 (NIR, 725-1100 nm), and thus fail to represent full optical range spectra. In addition,

25 it is worth pointing out that the stem optical properties are defined based on dead leaves estimates reported by Dorman and Sellers (1989). Additional confusion may be caused by the fact that the SiB-table by Dorman and Sellers (1989) defines NIR region as 700-4000 nm, whereas in one of the SiB-table source datasets (in Sellers, 1985) the respective wavelength region is defined as 700-3000 nm. Noteworthy is that the current standard of measuring spectral data extends only to 2500 nm. Although the spectral range used in this study does not cover the full theoretical range of total shortwave broadband albedo (300-4000

30 nm), the spectral range of 400-2400 nm contains ~96 % of the total solar irradiation (Thuillier et al., 2003, **Fig. 1.**) and thus suffices to approximate total VIS and NIR albedos. In addition, as the CLM-table contains a column for χ_L, we assess their appropriateness based on measured and published data. In CLM5, the predefined angles (χ_L, **Table 1.**) are 0.01 (~59.7°) for

both NETs, 'NDT boreal', 'BDT tropical' and 'BES temperate', 0.10 (~56.6°) for BETs, 0.25 (~51.3°) for BDT(/S) (refers to 'BDT+BDS') boreal and temperate, -0.3 (~69.5°) for grasses and C3 crops, and -0.5 (~75.5°) for other crops. As the focus of this paper is in optical properties, extensive review of leaf angle literature is not attempted.

5   **Table 1. User-friendly version of the CLM5 optical properties table in CLM5 (2018), manual (Table 2.8). Note, in CLM the leaf angle definition (χ_L) is quantified based on divergence from spherical distribution: 1=planophile, -1=erectophile, and 0=spherical. Reflectance (R) and transmittance (T) in VIS (<= 700 nm) and in NIR (>=701 nm). 'BDT(/S)' contains both BDT and BDS PFTs for temperate and boreal PFTs.**

Plant Functional Type (PFT)	χ_L	R (leaf, VIS)	R (leaf, NIR)	R (stem, VIS)	R (stem, NIR)	T (leaf, VIS)	T (leaf, NIR)	T (stem, VIS)	T (stem, NIR)
NET temperate; NET boreal; NDT boreal; BES temperate	0.01	0.07	0.35	0.16	0.39	0.05	0.10	0.001	0.001
BET tropical; BET temperate	0.10	0.10	0.45	0.16	0.39	0.05	0.25	0.001	0.001
BDT tropical	0.01	0.10	0.45	0.16	0.39	0.05	0.25	0.001	0.001
BDT(/S) temperate; BDT(/S) boreal	0.25	0.10	0.45	0.16	0.39	0.05	0.25	0.001	0.001
C3 arctic grass; C3 grass; C4 grass; C3 crop	-0.30	0.11	0.35	0.31	0.53	0.05	0.34	0.120	0.250
Temp corn; Spring wheat; Temp soybean; Cotton; Rice; Sugarcane; Tropical corn; Tropical soybean	-0.50	0.11	0.35	0.31	0.53	0.05	0.34	0.120	0.250

10   **2.2 Spectral databases**

Spectral repositories used in this study are openly available online archives that were selected based on their reputation and methods used to collect the data (e.g. device, spectral range, metadata availability). To reduce differences in data resulting from different instrumentation, we only used leaf/needle-level data measured using integrating sphere to get both leaf R and T information for forest and crop PFTs. For grasses 'canopy-level' R measurements were used (except for arctic grasses, for

15   which the data were collected using leaf clip) (**Table 2.**).

The Lopex93 and Angers datasets belong to a group of 'Foundational datasets' defined as "Previously published spectroscopic data and associated metadata resources that represent exemplary, historically-notable, or transformational collections for the environmental spectroscopy community" (EcoSIS, 2017). Lopex93 and Angers contains measurements of species with flat leaves, i.e., grasses, crops, broadleaved tree and shrub species. The Lopex93 campaign was organized by Joint Research Centre

5 (JRC) in Italy during the summer of 1993 and contains leaf R and T data for leaves of 45 species. Angers is a dataset collected by National Institute for Agricultural Research (INRA) in France on June 2003 containing R and T data for leaves from 39 species. For conifer needles few spectra are available due to obvious difficulties in measuring small needles. For boreal tree species two datasets are available by Lukeš et al. (2013) and Hovi et al. (2017) via SPECCHIO. For example, dataset by Hovi et al. (2017) contain R and T data for 25 Eurasian and North American boreal tree species measured during peak-growing

10 season. These two datasets contain measurements of both sun exposed and shaded leaves, by leaf sides (=adaxial and abaxial) from different canopy positions. For temperate conifers we used EcoSIS library from Serbin (2014) and data by Noda et al. (2014) stored in Japan Long-Term Ecological Research Network (JaLTER) archive. The dataset by Serbin (2014) was collected in the north-central and northeastern United States (US) as part of NASA Forest Functional Types Project (NNX08AN31G). The data from Noda et al. (2014) were measured in Japan with varying spectral ranges of 350-2500 nm and

15 350-2050 nm for foliage and barks (Note, spectra is available for leaves and shoots for different canopy positions; for foliage, the R and T are provided separately for abaxial and adaxial sides).

Bark R dataset was compiled using spectra from Noda et al. (2014), Hall et al. (1996), and Lang et al. (2002). In addition of containing bark R spectra, the Hall et al. (1996) dataset includes also measurements of branches, moss, and litter for boreal

20 conditions (collected in Superior National Forest of Minnesota US). However, in this study we used dataset by Lang et al. (2002), to assess variation in R of different C3 grass compositions because the spectral range of data from Lang et al. (2002) was larger than that of Hall's data. For arctic (C3) grasses we used EcoSIS data measured in Toolik, arctic research field station in Alaska (Toolik, 2017). For tropical (C4) grasses we used EcoSIS data 'Hawaii 2000' dataset (Dennison and Gardner, 2018). In the absence of measured transmittance data for grasses, it was assumed equal (in **Table S1**) with that of crops (and grasses)

25 contained by Lopex93 dataset.

30

Table 2. Spectral data used in this study. This table only lists data properties that were used in this study (i.e. the datasets may contain other data collected using different devices, methods or from different targets). Abbreviations: IS= integrating sphere, LC= leaf clip, BF= bare optical fibre or optical head of spectrometer, *R*= reflectance, and *T*= transmittance. Target 'BDT(/S)' contains both BDT and BDS PFTs for temperate and boreal regions, and similarly 'BET(/S)' contains both BET and BES PFTs.

Reference	Name	Area	Target	Wavelength region	Geometry, and measurements
Jacquemound et al., (2003)	Angers 2003	France	BDT(/S) temperate, BET(/S) temperate	400-2450 nm	IS, $R + T$
Hoosgood et al., (1993)	Lopex93	Italy	BDT(/S) temperate, BET(/S) temperate, Crops	400-2500 nm	IS, $R + T$
Lukeš et al., (2013)	NA	Finland	NET boreal, BDT(/S) boreal	400-2400 nm	IS, $R + T$
Hovi et al., (2017)	NA	Finland, Alaska	NET boreal, BDT(/S) boreal, NDT boreal	350-2500 nm, 400-2300 nm	IS, $R + T$
Noda et al., (2014)	NA	Japan	NET temperate, NDT boreal; Bark	350-2500 nm, 350-2050 nm	IS, $R + T$, BF, R
Serbin, (2014)	NA	USA	NET temperate	350-2500 nm	IS, $R + T$
Hall et al., (1996)	NA	USA	Bark	350-2100 nm	BF, R
Lang et al., (2002)	NA	Estonia, Sweden	C3 grass, Bark	400-2400 nm	BF, R
Toolik, (2017)	NA	Alaska	Arctic (C3) grass	350-2500 nm	LC, R
Dennison and Gardner, (2018)	Hawaii 2000	Hawaii	Tropical (C4) grass	350-2500 nm	BF, R

2.3 Processing of the spectra

The spectra from different repositories were resampled to follow constant spectral range and interval (i.e. the spectral range and measurement interval of different devices varies and must therefore be unified). Spectra were resampled to have 1 nm interval within a spectral range of 400-2400 nm using R-package 'Prospectr' (Stevens and Ramirez-Lopez, 2015). The spectral

10 regions with extreme noise were either removed or replaced with local means before smoothing. If 10% smoothing (span of 0.10) was enough to repair noisy regions in the spectra, no removals or replacements were done. Smoothing was done using loess regression (R default package) applying non-parametric least squares regression for localized subsets. Note, if spectra were available >2400 nm, it was removed in effort to harmonize the spectral range of the different data sets (**Table 2.**). Normalized solar irradiance (SI) spectra was used to weight both of *R* and *T* spectra before calculating the VIS (400-700 nm)

15 and NIR (701-2400 nm) averages for *R* and *T* (i.e. all band averages of *R* and *T* are given in after weighting with SI). We used the white-sky SI spectra measured at sea-level to account for atmospheric scattering and absorption effects (**Fig. 1.**). The SI spectra was normalized (i.e. to sum up to 1), separately for VIS and NIR wavelength bands (i.e. the relative shape of the SI spectra within the VIS and NIR subset was preserved). Foliage element single scattering albedo (*SSA*) spectra was obtained as a sum of *R* and *T* spectra (separately for VIS and NIR) and multiplied with the respectively (i.e. VIS or NIR) normalized SI

spectral curve. The leaf or needle *SSA* was obtained as a sum over the resulting VIS and NIR spectra. The SI normalization was adapted to shorter NIR spectral ranges of Hall et al. (1996), Hovi et al. (2017) and Noda et al. (2014) data (in **Table 2.**). All VIS and NIR -averaged *R*, *T* and *SSA* values represented in this paper have been weighted with the SI to show results consistently.
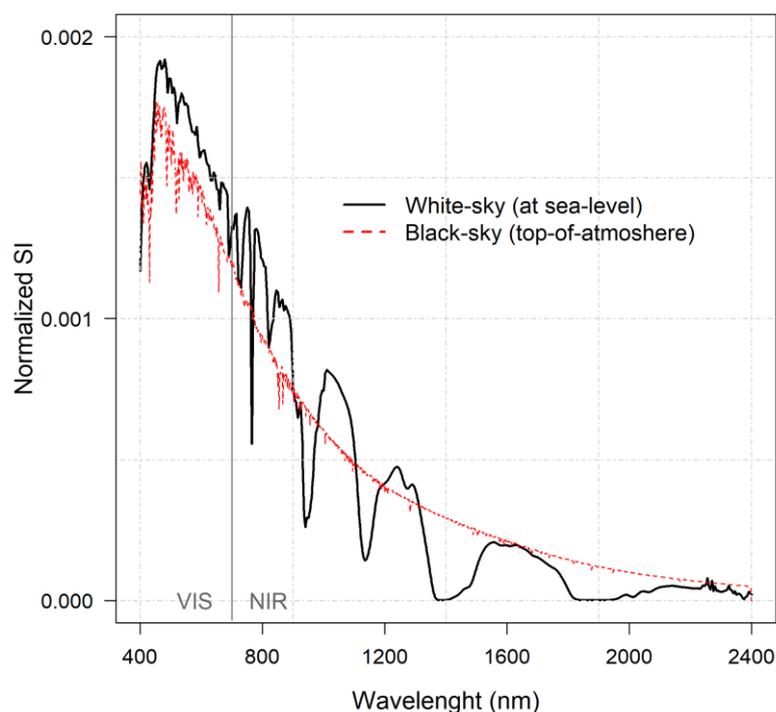
Figure 1. The normalized (i.e. sums to unity between 400-2400 nm) white-sky solar irradiance spectra (SI) measured at sea-level, and for a reference, the normalized black-sky top-of-the-atmosphere spectra by Thuillier et al. (2003). Figure is shown to illustrate the effect of atmosphere on the shape of SI spectral curves (Note, in our calculation the white-sky spectra was renormalized within VIS (400-700 nm) and NIR (701-2400 nm) subsets.

2.4 Upscaling from needle albedo to shoot albedo

Clustering of needles into shoots causes the *R* and *T* of shoots to be systematically smaller than that of needles, due to within-shoot multiple scattering (Stenberg, 1996). By replacing the VIS and NIR needle albedos with shoot albedos, the systematic bias caused by shoot-level clumping can be accounted for in RT modeling. The spectra of needles can be upscaled to shoot-level using spherically averaged Silhouette to Total needle Area Ratio (*STAR*, e.g. Oker-Blom and Smolander, (1988); Stenberg, (1996)). For a shoot without within-shoot shadowing, the *STAR* would be 0.25 because the spherically averaged projection area of a convex needle is one fourth of its total area (Lang, 1991). The *STAR* is known to vary between species and canopy positions (and may vary e.g. from 0.12 to 0.28), and in the absence of adequate data the *STAR* can be approximated

using a value of 0.16 for a range of shoot structures (Thérézien et al., 2007). In this study a constant *STAR* of 0.16 was used for all conifer species for demonstration. At shoot-level the p is linearly related with *STAR* (i.e. $p = 1 - 4 \times STAR$ under diffuse radiation conditions), which allows upscaling the *SSA* spectra ($SSA_{needle}, = R(\lambda) + T(\lambda)$) to shoot spectral albedo ($SSA_{(shoot)}$) (Smolander and Stenberg, (2003); Rautiainen et al., (2012)) as following Eq. (1):

$$SSA_{(shoot)(\lambda)} = SSA_{needle}(\lambda)\left(\frac{1-p}{1-pSSA_{needle}(\lambda)}\right) \tag{1}$$

The $SSA_{(shoot)}$ spectra were multiplied with normalized SI spectra for VIS and NIR wavelength regions as explained in **section 2.3**, and $SSA_{(shoot)}$ in VIS and NIR were obtained by taking the sum over the spectra.

2.5 Leaf angle specification

Leaf angle distribution (LAD) of foliage determines radiation transmission though plant canopies and is also included in the CLM5-table (in a form of χ_L). The assumption on random foliage distribution remains valid for many conifer species (e.g. Barclay, 2001), and thus we focus on providing some example data for other PFTs. The leaf angle properties of PFTs will be

15 defined based on data presented in Wang et al. (2007), Pisek et al., (2011, 2013), Gratani and Bombelli, (2000), Zou et al. (2014), and Campbell and Van Evert, (1994; reprinted in Campbell and Norman, 2012, pp.253).

Wang et al. (2007) reported measured *LIA*s for three grass species (i.e. *Andropogon gerardii*, *Panicum vigratum*, and *Sorghastrum nutans*) measured in Konza Prairie in North America (data from Li, 1994), and for leaves of 38 species including

20 flowering plants, shrubs and trees measured in Ku-ring-gai Chase National Park in Australia (data from Falster and Westoby, 2003). R-library 'RLeafAngle' (Wang et al. (2007), library updated June 20, 2017) contains two datasets, one called 'Pisek' which contains leaf angles for the 54 species measured at three European locations (i.e. Belgium, Estonia, and Britain) (used also in paper by Pisek et al. (2013)), and the second called 'Falster' for 38 species published by Falster and Westoby (2003). The Falster data were used to obtain *LIA* estimates for 'BDT(/S) tropical'. For 'BDT(/S) temperate' and 'BDT(/S) boreal' *LIA*

25 estimates were obtained from data by Pisek et al. (2011, 2013); Pisek et al. (2011) contains *LIA* estimates for four and Pisek et al. (2013) 54 temperate and boreal tree species. The mean *LIA* of 'BET(/S) temperate' and 'BET(/S) tropical' was approximated using two species from Hawai'i (i.e. *Metrosideros polymorpha*, and *Schizostachyum glaucifolium* (=bamboo) in Pisek et al. (2011)) and two from the Mediterranian region (i.e., *Phillyrea latifolia*, and *Quercus ilex*, in Gratani and Bombelli (2000)).

30

The variety of mean *LIA* estimates of different grass and crop species was demonstrated using data from Campbell and Van Evert (1994), Li (1994), and Zou et al. (2014). As it is not easy to classify different plant species into either crop or grass, we

chose to present these data by dataset (see **S3** for details). The pure 'Grasses' (Li, 1994) and cool-temperate 'Crops' (Zou et al., 2014) data contained measured *LIA* estimates, but 'Crops+Grass' data by Campbell and Van Evert (1994) were reported using ellipsoidal leaf angle distribution parameters '*x*' which needed to be converted to *LIA* in degrees (°). For this conversion we used the approximation: $LIA = -21.94 \times \log(x) + 58.63$, where *x* was the ratio of average projected area of canopy elements

5 on horizontal and vertical surfaces (Note, *LIA* conversion suggested by Campbell and Norman, (2012, pp.253) is not exact but suffices for our purpose). For each species in 'Crops+Grass' data, the mean *LIA* was obtained as the average of min and max *LIAs*; if min was not available, then max was used. The conversion between mean *LIA* (θ_{mean}) and χ_L was approximated following CLM5 (2018) manual as:

$$\cos \theta_{(mean)} = \frac{1+\chi_L}{2} \qquad (2)$$

For each PFT the mean *LIA* estimates in degrees and as dispersion from spherical (χ_L) were obtained as an average across species means (species level data listed in **S3**.). The species mean *LIA* estimates were assigned to classic LAD types (de Wit, 1965) using RLeafAngle -package function 'selectClassic()' and thus may differ from that presented in the original works.

15 **3 Results**

3.1 Forest PFTs

3.1.1 Optical properties of forest PFTs

The reflectance (*R*) and transmittance (*T*) of conifer needles were similar between 'NET temperate' and 'NET boreal' in both VIS and NIR wavelengths (**Fig. 2, Table 3.**). For example, for 'NET temperate' mean R_{VIS} was 0.08, and mean T_{VIS} was 0.04,

20 and for 'NET boreal' the respective values were 0.09 and 0.05. Similarly, for 'NET temperate' ('NET boreal') the mean R_{NIR} was 0.41 (0.41) and mean T_{NIR} was 0.31 (0.32). Thus, the R_{VIS} and T_{VIS} (0.07, 0.05) for NET appear appropriate in CLM (**Table 1.**). However, the CLM default *R* and *T* in NIR are not at the correct level: the CLM defaults for R_{NIR} and T_{NIR} are 0.35 and 0.10 - but based on our data the values should be ~0.41 and ~0.32, respectively.

25 The mean *R* and *T* were similar also for temperate and boreal BDTs (**Table 3.**). For 'BDT temperate', the mean R_{VIS} was 0.08 and mean T_{VIS} was 0.06, and for 'BDT boreal', the respective values were 0.09 and 0.05. Similarly, for 'BDT temperate' the mean R_{NIR} was 0. 42 and mean T_{NIR} was 0.43, while for 'BDT boreal' the respective values were 0.40 and 0.42. Thus, we can conclude that the CLM for BDT R_{VIS} and T_{VIS} are appropriate ($R_{VIS} = 0.10$ and $T_{VIS} = 0.05$). However, the CLM default value for 'BDT temperate and boreal' T_{NIR} of 0.25 requires an update: based on our data the respective T_{NIR} should be and ~0.43. For

30 R_{NIR} the CLM default is 0.45 and the mean measured estimate was ~0.41.

For BET temperate, the averages of R_{VIS} and T_{VIS} were 0.11 and 0.06, respectively (**Fig. 3c**, **Table 3.**). These values corresponded well with the CLM default values (i.e. R_{VIS}= 0.10 and T_{VIS}= 0.05). However, the CLM default T_{NIR} of 0.25 was slightly smaller than the mean measured T_{NIR} of 0.33). The CLM default BET R_{NIR} of 0.45 correspond well with the measured mean R_{NIR} of 0.46.

Results showed that the CLM optical properties for 'NDT boreal' are fine in VIS. However, CLM defaults for R_{NIR} and T_{NIR} of 0.35 and 0.10, were found too low – The R_{NIR} and T_{NIR} should be ~0.39 and ~0.42 based on measured data. Noteworthy is that, the 'NDT boreal' optical properties are more similar in NIR with BDT than with NET, which is the CLM default grouping (**Fig. 2.**).

Based on our simulations, the shoot albedos are on average 32% smaller in VIS and 11% smaller in NIR than the single scattering needle albedos (**Table 3.**, **S2**). The largest differences between the two albedo proxies resulted in a 36% difference in VIS and 15% difference in NIR, with the smallest differences being 29% in VIS and 7% in NIR.
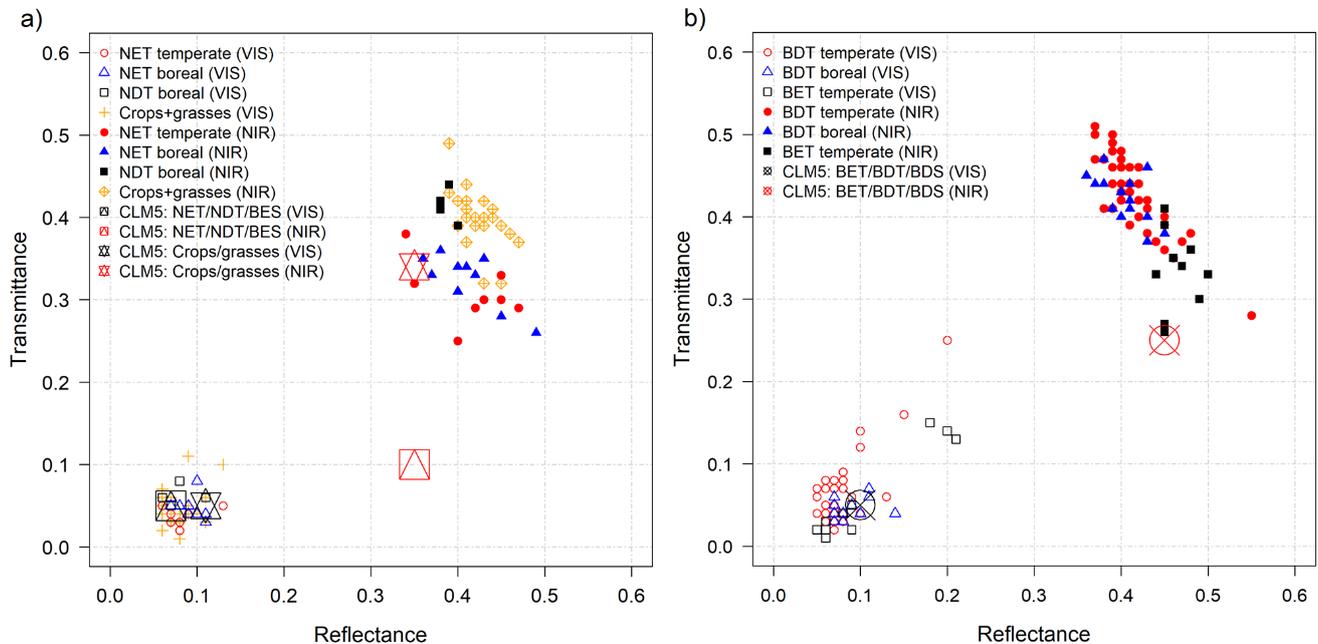
Figure 2. Leaf reflectance and transmittance in VIS (400-700 nm) and NIR (701-2400 nm) for different PFTs. Single species values are plotted to demonstrate the within- and between- PFT variation for a) 'NET temperate' and 'NET boreal', 'NDT boreal', and 'Crops+grasses', and b) 'BDT temperate' and 'BDT boreal', and 'BET temperate'. The CLM default optical properties are plotted using large symbols. For colors, please see the online version of the article.
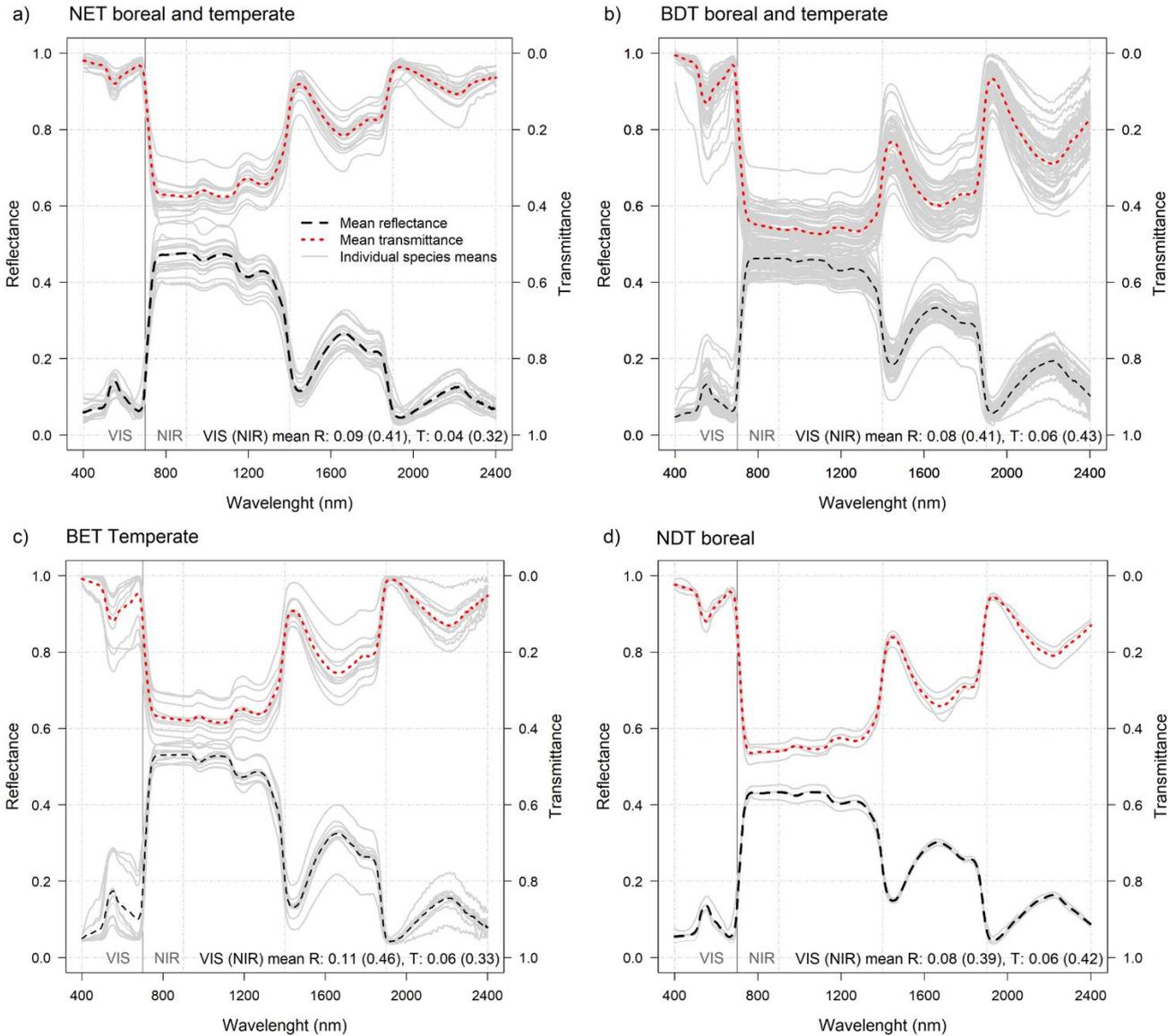
Figure 3. Average reflectance (*R*) and transmittance (*T*) spectra of foliage for forest Plant Functional Types (PFTs) for *n* species samples: a) NET boreal and temperate (n=18), b) BDT boreal and temperate (n=54), c) BET temperate (n=10), and d) NDT boreal (n=4). Individual species mean *R* and *T* spectra are shown using light grey lines and are used to represent the within PFT deviation in mean spectra (see individual species estimates in S2). The mean *R* and *T* for VIS (400-700 nm) and NIR (701-2400 nm) wavelengths are provided at the bottom of the images and are calculated as an average of the species means. Note, all VIS and NIR averages of *R* and *T* were weighted with solar irradiance spectra.

Table 3. Average leaf or needle reflectance (*R*), transmittance (*T*), single scattering albedo (*SSA*) and single scattering albedo corrected for shoot-level clumping (*SSA(shoot)*) over VIS (400-700 nm) and NIR (701-2400 nm) wavelength regions by Plant Functional Type (PFT). Note, all VIS and NIR averages of *R* and *T* were weighted with solar irradiance spectra.

PFT	R_{VIS}	T_{VIS}	SSA_{VIS}	$SSA(shoot)_{VIS}$	R_{NIR}	T_{NIR}	SSA_{NIR}	$SSA(shoot)_{NIR}$
NET temperate	0.08	0.04	0.12	0.08	0.41	0.31	0.72	0.64
NET boreal	0.09	0.05	0.14	0.10	0.41	0.32	0.74	0.66
NDT boreal	0.08	0.06	0.15	0.10	0.39	0.42	0.80	0.74
BET temperate	0.11	0.06	0.17		0.46	0.33	0.80	
BDT temperate	0.08	0.06	0.14		0.42	0.43	0.84	
BDT boreal	0.09	0.05	0.14		0.40	0.42	0.83	
Crop	0.08	0.05	0.13		0.42	0.40	0.82	

5 ### 3.1.2 Optical properties of tree bark
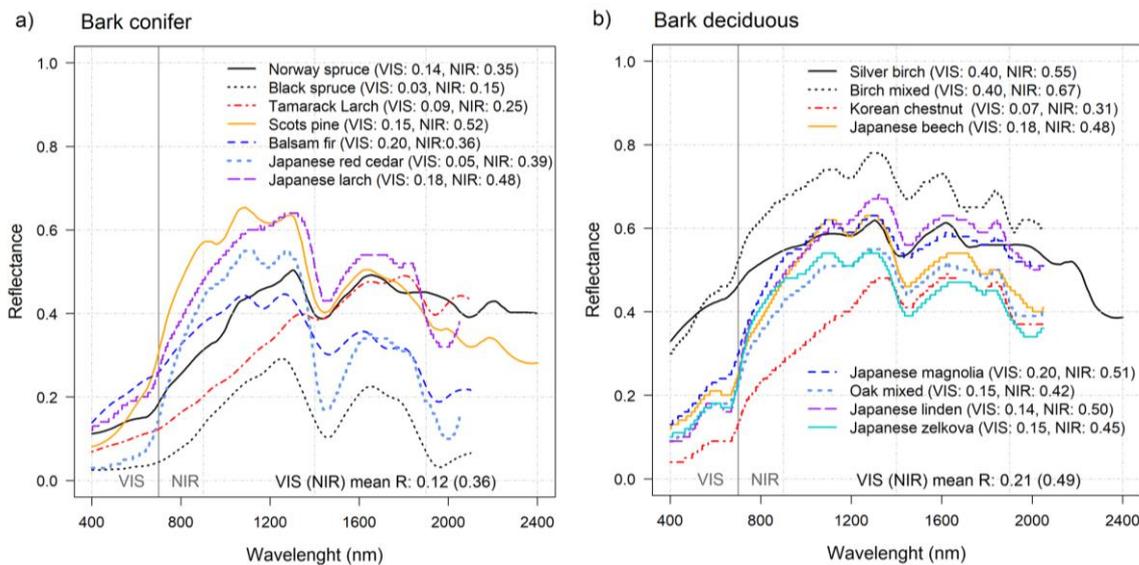
Figure 4. Bark reflectance (*R*) of a) coniferous, and b) deciduous species in VIS (400-700 nm) and NIR (701-2400 nm) wavelength regions. The mean bark reflectance values in VIS and NIR are provided at the bottom of the images and are calculated as an average across species means (the mean across all bark values R_{VIS} =0.17 and R_{NIR} = 0.43). Note, all VIS and NIR averages of *R* and *T* were
10 weighted with solar irradiance spectra. For colors, please see the online version of the article.

Based on our data sample, coniferous bark R_{VIS} varied between 0.03 and 0.20 and in R_{NIR} between 0.15 and 0.52 (Fig. 4a, S2). The average coniferous bark R_{VIS} was 0.12 and for R_{NIR} 0.36. For deciduous species, the bark R_{VIS} varied between 0.07 and 0.40, and in R_{NIR}, between 0.31 and 0.67 (Fig. 2b). The average deciduous species bark R_{VIS} and R_{NIR} were 0.21 and 0.49, respectively. In CLM, the same constant stem reflectance is used for all forested PFTs (R_{VIS} of 0.16 and R_{NIR} of 0.39). Thus,

the CLM default bark reflectance in VIS and NIR fall within the range of measured values (average over all species $R_{VIS} = 0.17$ and $R_{NIR} = 0.43$). However, alternatively bark reflectance could be defined separately for coniferous and deciduous PFTs.

3.2 Optical properties of grass and crop PFTs

[Figure 5 panels a)–d)]
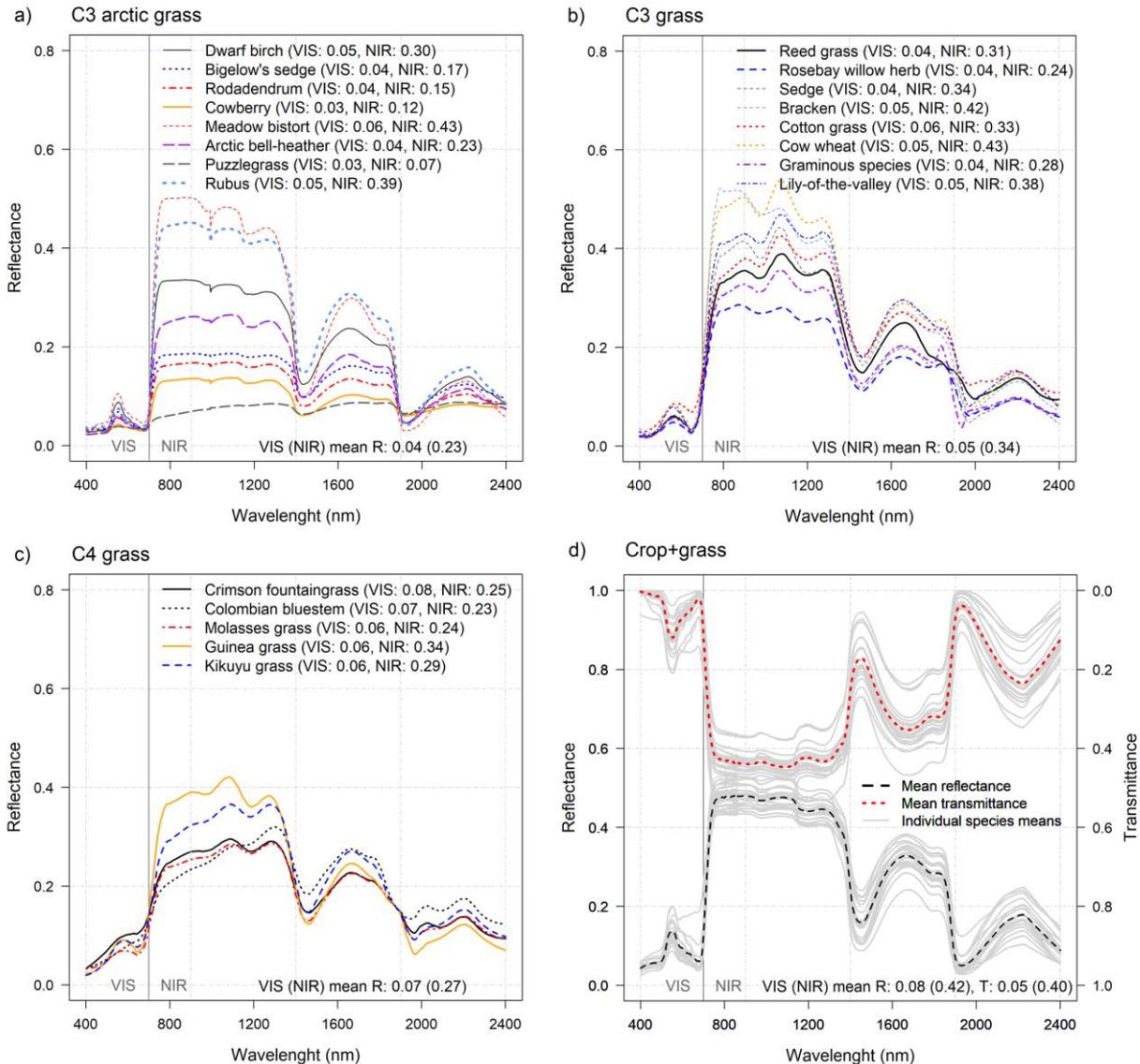
Figure 5. Optical properties of grasses and crops. Reflectance (R) of: a) C3 arctic grasses, b) C3 grass canopies, c) C4 grass canopies, and d) and transmittance (T) of leaves of different crops ($n=21$, contains also some grass species): Individual species mean R and T spectra are shown using light grey lines and are used to represent within PFT deviation in mean spectra (see individual species values in S2). The mean R and T for VIS (400-700 nm) and NIR (701-2400 nm) wavelengths are provided at the bottom of the images and are calculated as an average across species means. Note, all VIS and NIR averages of R and T were weighted with solar irradiance spectra. For colors, please see the online version of the article.

Reflectance spectra for different grass species demonstrates large within-PFT variation, which exceeds the differences between various grass PFTs (i.e. C4, C3 arctic, and C3 grasses). The mean R_{VIS} (T_{VIS}) of the different grass and crop types (i.e. C3 arctic grass, C3 grass, C4 grass, and crops were: 0.04 (0.23), 0.05 (0.34), 0.07 (0.27), and 0.08 (0.42), respectively (**Fig. 5.**, **S2**). In

5   the CLM table, the default R_{VIS} and R_{NIR} are 0.11 and 0.35 for all grass and crop PFTs. The CLM default R_{VIS} seems a little high as only 3/42 grass or crop species (i.e. garden lettuce, corn and soybean) reach the R_{VIS} of 0.11. The R_{NIR} of 0.35 on the other hand stands out like an outlier (**Fig. 2a.**, **S2**), and thus slightly higher value could be used. For crops, the measured mean T_{VIS} and T_{NIR} was 0.05 and 0.40, respectively. Thus, although the measured T_{VIS} values aligned perfectly with the CLM default value (of 0.05), the CLM default T_{NIR} value of 0.34 needs an update. For grasses the updated R_{VIS} and R_{NIR} could be ~0.05 and

10 ~0.28, and for crops ~0.08 and ~0.42 (**S2**). In the absence of measured transmittance data for grasses, the T_{VIS} and T_{NIR} of grasses could be defined based on respective crop values (i.e. 0.05 and 0.40).

3.3 Leaf angle specification

Based on measured data, the mean *LIA* of 'BDT tropical' (χ_L of 0.20 i.e. ~52.1°) was found more planophile than what is the

15 CLM default value of 0.01 (χ_L, i.e ~60°) (**Table 4, S3**). However, as there is a lot of variation among *LIA* estimates between species (i.e. χ_L ranges from -0.42 to 0.84), the assumption on spherical foliage orientation seems fine for 'BDT tropical'. For 'BDT(/S) temperate/boreal' the mean *LIA* across species means was 36.9° (i.e. χ_L of ~0.57) and, thus was also found more planophile than the CLM5 default of ~51.3° (i.e. χ_L of 0.25). Consequently, the χ_L value of 'BDT(/S) temperate/boreal' could be adjusted to correspond better with observed variation in the data. For 'BET(/S) temperate/tropical' the mean *LIA* was 48.5°

20 (i.e. χ_L of 0.32) and thus somewhat agreeing with the CLM5 default of ~56.6° (χ_L of 0.10).

Table 4. Mean leaf inclination angles (*LIA*s) of different flat-leaved Plant Functional Types (PFTs). The angles are provided both in degrees (°) and as departures from spherical (χ_L). Number of observations is shown in column '*n*'. Individual species estimates are presented in supplement S3.

PFT	Mean(°)	Sd(°)	Min(°)	Max(°)	Mean(χ_L)	Sd(χ_L)	Min(χ_L)	Max(χ_L)	n
BDT(/S) tropical	52.1	12.4	23.2	73.0	0.20	0.33	-0.42	0.84	38
BDT(/S) temperate/boreal	36.9	10.2	18.1	64.4	0.57	0.23	-0.14	0.90	58
BET(/S) temperate/tropical	48.5	6.2	43.5	57.1	0.32	0.17	0.09	0.45	4
Grass	67.4	5.5	61.3	72.7	-0.23	0.18	-0.41	-0.04	5
Crops (cool-temperate)	41.2	18.3	17.6	63.2	0.44	0.41	-0.10	0.91	6
Crops+Grass	48.2	7.9	34.3	63.3	0.32	0.21	-0.10	0.65	21

25

For the non-forest PFTs (i.e. grasses and crops), the CLM5 default parameterization of χ_L was either -0.30 (~69.5°) or -0.50 (~75.5°) depending on vegetation type. Based on measured data the mean χ_L of grasses (of -0.23, ~67.4°) was found to corresponding well with the CLM5 default value. However, for crops the observed χ_L values were clearly leaning towards

more planophile (e.g. 41.2° and 48.2°, χ_L of 0.44 and 0.32) than erectophile foliage orientation (i.e. ~75.5°, χ_L of -0.5). Cool-temperate crops demonstrated the largest variation in *LIA*s (ranged from 17.6° to 63.2°, i.e. χ_L from of -0.10 to 0.91). Noteworthy is that from among 32 grass and crops species, none reached χ_L of -0.50; however two grasses had χ_L of -0.40 (**Table 4**, **S3**). Thus, based on the data shown in this study, the CLM5 default χ_L of crops should be updated. The mean χ_L of

5   the crop species presented here was 0.34 (~46.6°) (**S3**).

4. Discussion

Based on a dataset compiled following a synthesis and harmonization of spectral data found in a variety of data repositories, we showed that many optical properties based on the 'SiB-table' (currently used by e.g. CLM) need an update. We cannot

10   argue that the values presented in this paper are the 'truth' *per se*, nor that the researchers should use the values presented in this paper. However, we can state that there are systematic biases in the optical property values in the NIR wavelength region, across all PFTs. For example, for NET and NDT the empirically based needle *SSA* values exceeded the CLM-default parameters by 62% and 78% - even after accounting shoot-level clumping, the $SSA(shoot)_{NIR}$ was still 44.4% (NET) and 64.4% (NDT) larger than the CLM defaults. Similarly, for the BDT, BET and crop PFTs the measured leaf SSA_{NIR} values were 20.0%,

15   14.3% and 18.8% larger than the CLM default estimates. Thus, we can argue that there is a need to update the parameters. As optical properties represent the effective surface variables required in land surface modeling, the changes in initial parameterization may be expected to result in changes in predicted surface fluxes. While the optical properties were by default at the correct level in VIS wavelength region (determines vegetation productivity *via* photosynthesis), the changes in optical properties in the NIR wavelength region will have an impact on predicted surface fluxes *via* changes in surface albedo and the

20   shortwave surface radiation budget. These findings support actions to revisit and update the optical properties currently used in different LSMs. To our knowledge, only Gottlicher et al. (2011) made an attempt to verify the CLM optical parameters of 'BET tropical' (PFT) using measured spectral data. However, as their NIR data covered only a part of the spectrum (from 701 -1300 nm), only VIS verification was obtained. Next step in enhancing the optical properties description in LSMs should focus on developing temporal routines for scaling optical property values based on vegetation growth and senescence (Yuan et al.,

25   2017).

PFT definitions are needed by LSMs to classify species into groups of similar structural and functional characteristics. While that appears a relatively simple task, this is not always the case. For example, while the difference between tree and a shrub might seem easy to define, in practice defining these two is complicated by overlapping definitions. While both trees and

30   shrubs are perennial woody plants, a shrub is considered shorter in stature than a tree and typically has more stems. However, a shrub may have as few as one stem and be tall in stature (up to 3 or 4 meters in height) analogous to a small tree. Thus, the optical properties of shrub PFTs could be defined based on respective forest PFTs optical properties. In practice, we suggest that optical properties of e.g. 'BES temperate' be based on 'BET tropical' and 'BET temperate' instead of on 'NET

temperate/boreal' and 'NDT boreal' optical properties, which is the default CLM grouping. In addition, as the optical properties of the 'NDT boreal' are more like those of BDT (especially in NIR) than to NET which is the current CLM default grouping - the CLM could classify NDT into BDT group rather than NET. Further, pending the PFT-boundaries: Here we classified English ivy as belonging to 'BET(/S) temperate', despite it being an evergreen vine, and bamboo as 'BET(/S) temperate/tropical' (as it can reach up to 15 meters height and has flat-leaf structures), although it is flowering plant rather than a tree or shrub.

3D radiative transfer models cannot be run in dynamic global vegetation models due to computational constraints and thus simpler modeling approaches remain as the preferred option (Loew et al., 2014). However, the common turbid-medium assumption of foliage being infinitely small and randomly distributed point-like scatterers allows replacing the optical properties of the elements. Thus, the well-known phenomenon called 'within-shoot multiple scattering' which causes the reflectance of coniferous forests to be lower than that of forests with broadleaved trees (Rautiainen and Stenberg, 2005) can be resolved by simply replacing the foliage single-scattering albedos with the shoot-albedo values (see **S2**). Noteworthy is that, as LSMs are often run using PFT distributions obtained from remotely sensed landcover products, and as there are no possibilities for within-PFT species differentiation, the use of constant shoot-structural factor to upscale needle albedo to shoot albedo may be justified. However, for other applications having species information readily available, the species-specific shoot structural factors should be used. According to Rautiainen et al. (2012), shoot albedos are considerably smaller than needle albedos, and there is more variation in shoot spectra (coefficient of variation, CV, 8-21%) than in the needle spectra (VC 2-13%) due to the geometry of the shoot. In this study, the shoot albedos in VIS and NIR were ~30% and ~10% smaller than the needle albedos (note that a constant factor was used). The important role of shoot-level clumping correction has been acknowledged and is currently incorporated into different types of radiative transfer modeling schemes such as PARAS 'p' models (see review by Stenberg et al. (2016)), Forest Reflectance and Transmittance (FRT) model (Kuusk and Nilson, 2000), and the MODIS LAI/fPAR algorithm (Myneni et al., 1999). Thus, the next field of application could be in LSM.

Many of today's land surface models such as JSBACH (Reick and Gayler, 2017), JULES, and Organizing Carbon and Hydrology in Dynamic EcosystEms (ORCHIDEE) assume LAD to be spherical. However, the assumption of spherical LAD has been found to cause significant underestimation of light transmission (Stadt and Lieffers, 2000), and has been found to be invalid for most temperate and boreal deciduous tree species based on an extensive dataset of measured LADs (i.e. only 5 of 58 species the LAD was spherical (Pisek et al., 2013)). Another study with Australian species showed that only 3/12 types of herbaceous plant canopies and 8/38 plant species (e.g. trees, woody shrubs, climbers, ferns and cycads) had spherical LAD (Wang et al., 2007). Note that these two datasets were used also in this study. In CLM the LAD definition denotes the departure from spherical: Based on results the CLM default LAD definition of forested PFTs could be slightly more planophile. For LSMs which can implement non-spherical LAD definitions, LAD parameters for a range of species are readily available from Pisek et al., (2013) and Wang et al. (2007). However, the finding that CLM5 default LAD for crops is notably too vertical (i.e.

CLM5 default crop χ_L stands out as an outlier from among the empirical observations) requires attention from modelers. We acknowledge, that while LAD may be assumed a species-specific parameter, it may be hard to estimate correctly as it changes based on plant development stage (e.g. crops) and as a response to solar illumination conditions (i.e. dual role of being exposed for solar radiation to enable photosynthesis, but to avoid overexposure which would cause heat stress). Thus, future studies are needed to address the issue of the PFT LAD definition, especially in the case of grasses and crops that are more exposed to solar radiation than trees. As an alternative to field measurements, LAD may be also inverted based on remotely sensed data (Huang et al., 2006).

In the future, large databases which systematically collect chemical and spectral data at different scales (i.e. from leaf to canopy-level) and standardized protocols for field and lab work may be expected to become more common (e.g. Asner and Martin, 2016). While the motivation of remote sensing scientists is to build these databases to foster scientific discoveries, the same databases could also be used to provide inputs for different LSMs (especially those employing plant traits). The build-up of larger databases would solve most of present-day problems in terms of data usability by providing standardized data access policies, data formats, preprocessing, and metadata. We should aim for 'truthful' description of vegetation properties in different LSMs, as that is prerequisite for increasing the accuracy of the predictions.

Conclusions

Using the CLM PFT grouping as an example, we found the default PFT optical parameters appropriate in VIS band, but in NIR the updates are needed. Such updates may be expected to have direct impact in the modeling of surface albedo and the shortwave radiation balance. Thus, we encourage modelers employing two-stream RT approximations based on leaf-level optical properties to check their models' default optical properties parameters.

Code availability

No code available for this manuscript.

Data availability

Leaf angle datasets by Pisek et al. (2013) and Falster and Westoby, (2003) are available via available via RLeafAngle R-package (dataset names "Pisek" and "Falster"). Optical property estimates calculated from the raw data are included in SI. Raw spectral data is stored into openly available data repositories (listed in Table 2.):

Jacquemound et al., (2003):

https://ecosis.org/#result/2231d4f6-981e-4408-bf23-1b2b303f475e

Hoosgood et al., (1993):

https://ecosis.org/#result/13aef0ce-dd6f-4b35-91d9-28932e506c41

Lukeš et al., (2013):

Dataset name "OP_measurements" available via https://specchio.ch/

Hovi et al., (2017):

Dataset name "Hovi_et_al_2017_Silva_Fennica(Version1.0)" available via https://specchio.ch/

Noda et al., (2014):

5   http://db.cger.nies.go.jp/JaLTER/metacat/metacat?action=read&qformat=default&sessionid=&docid=ERDP-2013-02.1

Serbin, (2014):

https://ecosis.org/#result/4a63d7ed-4c1e-40a7-8c88-ea0deea10072

Hall et al., (1996):

https://daac.ornl.gov/cgi-bin/dsviewer.pl?ds_id=183

10   Lang et al., (2002):

https://www.aai.ee/bgf/ger2600/

Toolik, (2017):

https://ecosis.org/#result/1d0cb17c-0c0a-4775-8ca6-b8f2975b5041

Dennison and Gardner, (2018):

15   https://ecosis.org/#result/060d2822-f250-4869-b734-4a92450393f0

Supporting Information

The supplementary files of this article can be used to inspect the observed variation in both optical properties and leaf angles by species, and to recalculate the PFT means following different PFT definitions. Three supplementary files are provided: Our recommendation for enhancing CLM5 optical properties table ('S1_CLM5.pdf'), and two source files ('S2_OP.csv' and

5   'S3_LIA.csv'), which contain species mean optical properties (i.e. reflectance, transmittance and albedo values) values over the VIS and NIR bands, and species mean *LIA*s (in degrees and departure from spherical + classic leaf angle type) along with references to original data.

Author contribution

10 Majasalmi was responsible for the analysis and had a leading role in writing the paper. Bright participated in writing the paper.

Acknowledgements,

The research was funded by the Research Council of Norway, grant number 250113/F20. We thank Aarne Hovi, Miina Rautiainen, Nea Kuusinen, Petr Lukeš and Pauline Stenberg for helpful discussions.

15 **References**

Asner, G. P. and Martin, R. E.: Spectranomics: Emerging science and conservation opportunities at the interface of biodiversity and remote sensing, Glob. Ecol. Conserv., doi:10.1016/j.gecco.2016.09.010, 2016.

Asner, G. P., Wessman, C. A., Schimel, D. S. and Archer, S.: Variability in leaf and litter optical properties: Implications for BRDF model inversions using AVHRR, MODIS, and MISR, Remote Sens. Environ., doi:10.1016/S0034-4257(97)00138-7,

20 1998.

Barclay, H. J.: Distribution of leaf orientations in si× conifer species, Can. J. Bot., 79(4), 389–397, doi:10.1139/cjb-79-4-389, 2001.

Bonan, G. B., Oleson, K. W., Vertenstein, M., Levis, S., Zeng, X., Dai, Y., Dickinson, R. E. and Yang, Z. L.: The land surface climatology of the community land model coupled to the NCAR community climate model, J. Clim., 15(22), 3123–3149,

25 doi:10.1175/1520-0442(2002)015<3123:TLSCOT>2.0.CO;2, 2002.

Campbell, G. S. and Van Evert, F. K.: Light interception by plant canopies: efficiency and architecture. JL Monteith, RK Scott and MH Unsworth, Resource Capture by Crops. Nottingham University Press, Nottingham., 1994.

Campbell, G. S. and Norman, J. M.: An introduction to environmental biophysics. Springer Science & Business Media., 2012.

Clark, D. B., Mercado, L. M., Sitch, S., Jones, C. D., Gedney, N., Best, M. J., Pryor, M., Rooney, G. G., Essery, R. L. H.,

30 Blyth, E., Boucher, O., Harding, R. J., Huntingford, C. and Cox, P. M.: The Joint UK Land Environment Simulator (JULES), model description – Part 2: Carbon fluxes and vegetation dynamics, Geosci. Model Dev., 4(3), 701–722, doi:10.5194/gmd-4-701-2011, 2011.

CLM5: Community Land Model 5. CLM5 manual (https://escomp.github.io/ctsm-docs/doc/build/html/tech_note/index.html),

2018.

Combal, B., Baret, F., Weiss, M., Trubuil, A., Macé, D., Pragnère, A., Myneni, R., Knyazikhin, Y. and Wang, L.: Retrieval of canopy biophysical variables from bidirectional reflectance using prior information to solve the ill-posed inverse problem, Remote Sens. Environ., doi:10.1016/S0034-4257(02)00035-4, 2003.

5 Dennison, P. E. and Gardner, M. E.: Hawaii 2000 vegetation species spectra. Data set. Available on-line [http://ecosis.org] from the Ecological Spectral Information System (EcoSIS). doi:10.21232/C2HT0K, https://ecosis.org/#result/060d2822-f250-4869-b734-4a92450393f0, 2018.

Dorman, J. and Sellers, P.: A Global Climatology of Albedo, Roughness Length and Stomatal Resistance for Atmospheric General …, J. Appl. Meteorol., 28, 833–855, doi:10.1175/1520-0450(1989)028<0833:AGCOAR>2.0.CO;2, 1989a.

10 Dorman, J. L. and Sellers, P. J.: A Global Climatology of Albedo, Roughness Length and Stomatal Resistance for Atmospheric General Circulation Models as Represented by the Simple Biosphere Model (SiB), J. Appl. Meteorol., doi:10.1175/1520-0450(1989)028<0833:AGCOAR>2.0.CO;2, 1989b.

EcoSIS: EcoSIS Spectral library. http://ecosis.org/., 2017.

Falster, D. S. and Westoby, M.: Leaf size and angle vary widely across species: What consequences for light interception?,
15 New Phytol., doi:10.1046/j.1469-8137.2003.00765.x, 2003.

Gates, D. M., Keegan, H. J., Schleter, J. C. and Weidner, V. R.: Spectral Properties of Plants, Appl. Opt., doi:10.1364/AO.4.000011, 1965.

Gottlicher, D., Albert, J., Nauss, T. and Bendix, J.: Optical properties of selected plants from a tropical mountain ecosystem – Traits for plant functional types to parametrize a land surface model, Ecol. Modell., doi:10.1016/j.ecolmodel.2010.09.021,
20 2011.

Goudriaan, J.: The bare bones of leaf-angle distribution in radiation models for canopy photosynthesis and energy exchange, Agric. For. Meteorol., doi:10.1016/0168-1923(88)90089-5, 1988.

Gratani, L. and Bombelli, A.: Correlation between leaf age and other leaf traits in three Mediterranean maquis shrub species : Quercus ilex , Phillyrea latifolia and Cistus incanus, , 43, 141–153, 2000.

25 Gu, L., Baldocchi, D., Verma, S. B., Black, T. A., Vesala, T., Falge, E. M. and Dowty, P. R.: Advantages of diffuse radiation for terrestrial ecosystem productivity, , 107, 2002.

Hall, F. G., Huemmrich, K. F., Strebel, D. E., Goetz, S. J., Nickeson, J. E. and Woods., K. D.: SNF Leaf Optical Properties: Cary-14. ORNL DAAC, Oak Ridge, Tennessee, USA. https://daac.ornl.gov/SNF/guides/leaf_optical_properties_cary14.html, https://doi.org/10.3334/ORNLDAAC/183, 1996.

30 Hosgood, B., Jacquemoud, S., Andreoli, G., Verdebout, J., Pedrini, A., & Schmuck, G.: Leaf Optical Properties Experiment Database (LOPEX93). Data set. Available on-line [http://ecosis.org] from the Ecological Spectral Information System (EcoSIS), 1993.

Hovi, A., Raitio, P. and Rautiainen, M.: A spectral analysis of 25 boreal tree species, , 51(4), 1–16, 2017.

Huang, W., Niu, Z., Wang, J., Liu, L., Zhao, C. and Liu, Q.: Identifying Crop Leaf Angle Distribution Based on Two-Temporal

and Bidirectional Canopy Reflectance, , 44(12), 3601–3609, 2006.

Hueni, A., Nieke, J., Schopfer, J., Kneubühler, M. and Itten, K. I.: The spectral database SPECCHIO for improved long-term usability and data sharing, Comput. Geosci., 35(3), 557–565, 2009.

Jacquemound, S., Bidel, L., Francois, C., Pavan, G.: ANGERS Leaf Optical Properties Database (2003). Data set. Available on-line [http://ecosis.org] from the Ecological Spectral Information System (EcoSIS), 2003.

Knapp, A. K. and Carter, G. A.: Variability in leaf optical properties among 26 species from a broad range of habitats, Am. J. Bot., doi:10.2307/2446360, 1998.

Kuusk, A. and Nilson, T.: A Directional Multispectral Forest Reflectance Model, , 252(December 1999), 244–252, 2000.

Lang, A. R. G.: Application of some of Cauchy's theorems to estimation of surface areas of leaves, needles and branches of plants, and light transmittance, Agric. For. Meteorol., doi:10.1016/0168-1923(91)90062-U, 1991.

Lang, M., A., K., T., Nilson, T., . L., M., P. and G., A.: Reflectance spectra of ground vegetation in sub-boreal forests, Tartu Obs. Est. 8. http//www.aai.ee/bgf/ger2600/, 2002.

Li, Y.: Leaf Angle Data (FIFE). ORNL DAAC, Oak Ridge, Tennessee, USA. https://doi.org/10.3334/ORNLDAAC/44, 1994.

Loew, A., Bodegom, P. M. Van, Otto, J., Quaife, T., Pinty, B., Raddatz, T., Commission, E., Joint, S., Via, E. and Gate, E.: Do we (need to) care about canopy radiation schemes in DGVMs ? Caveats and potential impacts, , 1873–1897, doi:10.5194/bg-11-1873-2014, 2014.

Lukeš, P., Stenberg, P., Rautiainen, M., Mõttus, M. and Vanhatalo, K. M.: Optical properties of leaves and needles for boreal tree species in Europe, Remote Sens. Lett., 4(7), 667–676, doi:10.1080/2150704X.2013.782112, 2013.

Middleton, E. M., Sullivan, J. H., Bovard, B. D., Deluca, A. J., Chan, S. S. and Cannon, T. A.: Seasonal variability in foliar characteristics and physiology for boreal forest species at the five Saskatchewan tower sites during the 1994 Boreal Ecosystem-Atmosphere Study, J. Geophys. Res., doi:10.1029/97JD02560, 1997.

Miller, L. D.: Passive remote sensing of natural resources. Dept. of Watershed Science, Colorado State University, Colorado., 1972.

Myneni, R. B., Knyazikhin, Y., Privette, J. L., Running, S. W., Nemani, R., Zhang, Y., Tian, Y., Wang, Y., Morissette, J. T., Glassy, J. and Votava, P.: MODIS Leaf Area Index (LAI) And Fraction Of Photosynthetically Active Radiation Absorbed By Vegetation (FPAR) Product, Modis Atbd, Version 4., 130, doi:http://eospso.gsfc.nasa.gov/atbd/modistables.html, 1999.

Nilson, T. and Ross, J.: Modeling radiative transfer through forest canopies: implications for canopy photosynthesis and remote sensing, in The Use of Remote Sensing in the Modeling of Forest Productivity., 1996.

Noda, H. M., Motohka, T., Murakami, K., Muraoka, H. and Nasahara, K. N.: Reflectance and transmittance spectra of leaves and shoots of 22 vascular plant species and reflectance spectra of trunks and branches of 12 tree species in Japan, Ecol. Res., doi:10.1007/s11284-013-1096-z, 2014.

Norman, J. M., & Jarvis, P. G.: Photosynthesis in Sitka spruce (Picea sitchensis (Bong.) Carr.): V. Radiation penetration theory and a test case, J. Appl. Ecol., 839–878, 1975.

Oker-Blom, P., & Kellomäki, S.: Effect of angular distribution of foliage on light absorption and photosynthesis in the plant

canopy: theoretical computations, Agric. Meteorol., 26(2), 105–116, 1982.

Oker-Blom, P. and Smolander, H.: The Ratio of Shoot Silhouette Area to Total Needle Area in Scots Pine, For. Sci., 1988.

Pisek, J., Ryu, Y. and Alikas, K.: Estimating leaf inclination and G-function from leveled digital camera photography in broadleaf canopies, Trees, doi:10.1007/s00468-011-0566-6, 2011.

5 Pisek, J., Sonnentag, O., Richardson, A. D. and Mõttus, M.: Is the spherical leaf inclination angle distribution a valid assumption for temperate and boreal broadleaf tree species?, Agric. For. Meteorol., doi:10.1016/j.agrformet.2012.10.011, 2013.

Rautiainen, M. and Stenberg, P.: Application of photon recollision probability in coniferous canopy reflectance simulations, Remote Sens. Environ., doi:10.1016/j.rse.2005.02.009, 2005.

10 Rautiainen, M., Mõttus, M., Yáñez-rausell, L., Homolová, L. and Schaepman, M. E.: Remote Sensing of Environment A note on upscaling coniferous needle spectra to shoot spectral albedo, , 117, 469–474, doi:10.1016/j.rse.2011.10.019, 2012.

Reick, C. H. and Gayler, V.: JSBACH 3 — The land component of the MPI Earth System Model, 2017.

Reick, C. H., Gayler, V. and Raddatz, T.: The new land component of ECHAM, 2012.

Ridder, K.: Radiative transfer in the IAGL land surface model, J. Appl. Meteorol., 36(1), 12–21, 1997.

15 Ryu, Y., Sonnentag, O., Nilson, T., Vargas, R., Kobayashi, H., Wenk, R. and Baldocchi, D. D.: Agricultural and Forest Meteorology How to quantify tree leaf area index in an open savanna ecosystem : A multi-instrument and multi-model approach, , 150, 63–76, doi:10.1016/j.agrformet.2009.08.007, 2010.

Sellers, P. J.: Canopy reflectance, photosynthesis and transpiration, Int. J. Remote Sens., doi:10.1080/01431168508948283, 1985.

20 Serbin, S.: Fresh Leaf Spectra to Estimate Leaf Morphology and Biochemistry for Northern Temperate Forests. Data set. Ecological Spectral information Systems (EcoSIS), USA, 2014. http://ecosis.org/, 2014.

Smolander, S. and Stenberg, P.: A method to account for shoot scale clumping in coniferous canopy reflectance models, , 88, 363–373, doi:10.1016/j.rse.2003.06.003, 2003.

Smolander, S. and Stenberg, P.: Simple parameterizations of the radiation budget of uniform broadleaved and coniferous
25 canopies, , 94, 355–363, doi:10.1016/j.rse.2004.10.010, 2005.

Stadt, K. J. and Lieffers, V. J.: MIXLIGHT : a flexible light transmission model for mixed-species forest stands, , 102, 235–252, 2000.

Stenberg, P.: Correcting LAI-2000 estimates for the clumping of needles in shoots of conifers, Agric. For. Meteorol., doi:10.1016/0168-1923(95)02274-0, 1996.

30 Stenberg, P., Mõttus, M. and Rautiainen, M.: Photon recollision probability in modelling the radiation regime of canopies - A review, Remote Sens. Environ., doi:10.1016/j.rse.2016.05.013, 2016.

Stevens, A. and Ramirez-Lopez, L.: Package 'prospectr: Miscellaneous functions for processing and sample selection of vis-NIR diffuse reflectance data. Version 0.1.3, Date 2013-12-11., 2015.

Thérézien, M., Palmroth, S., Brady, R. and Oren, R. A. M.: Estimation of light interception properties of conifer shoots by an

improved photographic method and a 3D model of shoot structure, , 1, 1375–1387, 2007.

Thuillier, G., Hersé, M., Labs, D., Foujols, T., Peetermans, W., Gillotay, D., Simon, P. C. and Mandel, H.: The solar spectral irradiance from 200 to 2400 nm as measured by the SOLSPEC spectrometer from the ATLAS and EURECA missions, Sol. Phys., doi:10.1023/A:1024048429145, 2003.

5   Toolik: Alaska Plant Species Leaf Reflectance Spectra (SVC). Data set. Available on-line [http://ecosis.org] from the Ecological Spectral Information System (EcoSIS), 2017.

Wang, W., Li, Z. and Su, H.: Comparison of leaf angle distribution functions : Effects on extinction coefficient and fraction of sunlit foliage, , 143, 106–122, doi:10.1016/j.agrformet.2006.12.003, 2007.

Warren Wilson, J.: Inclined point quadrats., New Phytol., 59(1), 1–7, 1960.

10   Wit, C. T. de: Photosynthesis of leaf canopies., 1965.

Yuan, H., Dai, Y., Dickinson, R. E., Pinty, B., Shangguan, W., Zhang, S., Wang, L. and Zhu, S.: Reexamination and further development of two-stream canopy radiative transfer models for global land modeling, J. Adv. Model. Earth Syst., doi:10.1002/2016MS000773, 2017.

Zou, X., Mõttus, M., Tammeorg, P., Lizarazo, C., Takala, T., Pisek, J., Mäkelä, P., Stoddard, F. L. and Pellikka, P.: Agricultural

15   and Forest Meteorology Photographic measurement of leaf angles in field crops, Agric. For. Meteorol., 184, 137–146, doi:10.1016/j.agrformet.2013.09.010, 2014.